To be submitted to: AIAA J. of Thermophysics and Heat Transfer

Direct Measurements of Eddy Transport and Thermal Dispersion in a High Porosity Matrix

Yi Niu[1] and Terry Simon[2]
University of Minnesota, Minneapolis, MN 55455

David Gedeon[3]
Gedeon Associates, Athens, OH 45701

Mounir Ibrahim[4]
Cleveland State University, Cleveland, OH 44115

Thermal losses from the hot end to the cold end of a Stirling cycle regenerator due to thermal dispersion through the regenerator matrix may significantly degrade the performance of the machine. Because of poor access to the void spaces within the porous medium, no direct measurements of thermal dispersion have been made and dispersion models have been derived indirectly. This is done by measuring the overall thermal performance of the regenerator and subtracting off the energy transfer caused by molecular conduction and advected enthalpy flows computed from volume-averaged fluid velocity and temperature. In the current program, a large-scale porous matrix consisting of stacked wire screens with a porosity of 90% is installed in a flow rig which is operated in a Reynolds number range that represents Stirling engine regenerator flow. Experiments are conducted to measure turbulent transport of momentum at the exit plane using hot-wires. The relationship of such turbulent transport terms to the thermal dispersion term in the volumetric-averaged energy equation for the regenerator matrix is developed and the measurements are used to determine cross-stream thermal dispersion. A dispersion model based upon the measurements is proposed and compared with models documented in the literature.

Nomenclature

C_p	=	specific heat of fluid phase, J/kg K
C_t	=	correlation coefficient
d	=	characteristic length, m
d_h	=	hydraulic diameter, m
K	=	permeability of porous matrix, m^2
$\boldsymbol{k_d}$	=	thermal dispersion conductivity, W/mK
k_f	=	thermal conductivity of fluid phase, W/mK
N	=	the number of points selected to evaluate eddy viscosity
Pe	=	Peclet number $= ud / \alpha_f$
r	=	radial locations, m
T	=	temperature, K

[1] Research Assistant, Department of Mechanical Engineering, 111 Church St. SE, MPLS, MN, 55455, AIAA Member
[2] Professor, Department of Mechanical Engineering, 111 Church St. SE, MPLS, MN, 55455, AIAA Member.
[3] Consultant, Gedeon Associates, 16922 South Canaan Road, Athens, OH, 45701, AIAA Member.
[4] Professor, Department of Mechanical Engineering, 1960 East 24th St., Cleveland, OH, 44115, AIAA Associate Fellow.

u = velocity, m/s
α_f = thermal diffusivity of fluid phase, m^2/s
ε_d = thermal dispersion eddy diffusivity, m^2/s
ε_M = eddy diffusivity of momentum, , m^2/s
λ = dispersion coefficient
ρ = density of fluid phase, kg/m^3
σ = anisotropy factor

Introduction

Porous materials have been widely used for regeneration of engines, such as Stirling engines. Typically, the Stirling engine regenerators are made of wire screens or random fibers. The regenerator allows the ideal Stirling cycle machine to have a cycle efficiency equal to the Carnot cycle efficiency. Regenerator flow losses and heat transfer through the matrix contribute significantly to degrade the performance of the Stirling cycle, however. An important degradation mode is via the net energy flux through the regenerators directly to the coolers.[1] It was noted that a 1% decrease in energy storage in an engine regenerator matrix might necessitate a 4~5% increase in thermal energy input to a heater (i.e. a 4~5% decrease in efficiency), assuming the same indicated power. A major contribution to this energy transfer has become known as enhancement in axial heat conduction due to dispersion within the working gas (a component of which is due to eddy diffusion). It is a result of interaction of the flow with the regenerator matrix.

In porous media, "dispersion" is described as "heat transfer due to hydrodynamic mixing of the interstitial fluid at the pore scale."[2] It can be derived from the energy equation using volume averaging techniques and is defined as a correlation of the spatial fluctuations of temperature and velocity. For a flow with a high Peclet number, the thermal dispersion conductivity tensor, $\boldsymbol{k_d}$, can be modeled as

$$\boldsymbol{k_d} = \lambda k_f Pe \tag{1}$$

The dimensionless parameter, λ , called the dispersion coefficient, depends on the structure of the porous medium, the flow structure and the flow direction. However, for a homogeneous isotropic porous matrix, the component of thermal dispersion due to eddy transport might be isotropic and a main contributor of the thermal dispersion in cross-stream direction. The eddy component of dispersion is the focus of the present paper.

Extensive investigations have experimentally and theoretically determined the dispersion coefficient. A majority of the research has focused on a packed-particle bed since it is a simulation of many of porous media in nature. For this type of porous medium, Yagi and Kunni[3] determined the coefficient, λ , equal to 0.09~0.1. Hsu and Cheng[4] carried out experiments in cylindrical and annular tubes filled with glass spheres and derived the radial dispersion coefficient as a function of porosity. More recently, the radial dispersion coefficient was determined by Metzger et al.[5] to be about 0.03. For packed beds, the characteristic length, d, is the particle diameter.

The porous structures of Stirling regenerators (consisting of wire screen or random fibers) differ from those for a packed bed. Moreover, the regenerators have a high porosity (80~95%) compared to packed beds (less than 40%). Therefore, none of the above models should be used directly in Stirling regenerators. Koch and Brady[6] analytically derived models for fibrous media. Different expressions were given to calculate the coefficients in different flow regimes and dor different directions. Nakayama and Kuwahara[7] numerically modeled convective heat transfer through a number of square rods as microscopic structures of a porous medium and gave correlations of dispersion in both longitudinal and transverse directions. Both models include the porosity as a parameter. Hunt and Tien[8] measured heat transfer through a wall to porous media with porosities up to 97% and determined dipersion coefficients in that region to be about 0.025. They used the square-root of the permeability, $\sqrt{K}$, as the characteristic length. Few researchers have addressed modeling of dispersion in Stirling machines. Gedeon et al.[9] extracted axial dispersion coefficient from experiments taken under oscillatory flow conditions. Results were computed from the the fluid peak value of bulk mean velocity and the fluid average temperature over a cycle and overall heat losses. They derived correlations of effective axial conductivity for various porous structures commonly used in Stirling regenerators[9,10].

Kaviany[11] summarized different experimental methods to determine the thermal dispersion. The experimental methods frequently used (e.g. Ref. 5 and 8) require a solution of the macroscopic energy equation with the thermal dispersion coefficient included as a parameter. One can obtain the dispersion coefficient by matching the measured

temperatures or the measured heat transfer coefficients to those predicted by the solution. To the authors' knowledge, no efforts have been taken to assess thermal dispersion by measuring flow velocity and temperature at the pore level, directly. There exist two challenges. One is that due to the complex geometry of typical porous media, no access is available for any currently existing probes. The other challenge is that even we do have access, the evaluation of spatial correlations of flow and temperature fields requires a number of probes within the porous medium so that the readings are taken simultaneously. It does not seem practical. The present paper is attempting to evaluate the eddy component of dispersion by direct measurements. The spatial variations of the velocity and temperature fields are described in terms of temporal variations with the aid of the following theoretical approach.

Theoretical Approach

A volume averaging technique has been commonly used in porous media studies. Any microscopic quantity, W, can be decomposed into the sum of the volumetric average (macroscopic) quantity $\langle W \rangle$ integrated over a representative elementary volume (R.E.V.), and a spatial variation, $\tilde{W}$,

$$W = \langle W \rangle + \tilde{W} \tag{2}$$

where W and $\tilde{W}$ are functions of both time and space and $\langle W \rangle$ is a function of time, only. One can obtain one single volume-averaged energy equation by applying this technique to the energy equations for both solid and fluid phases while assuming thermal-equilibrium between the two phases,[4,7]

$$\rho_f C_p \langle \mathbf{u} \rangle \cdot \nabla \langle T \rangle = \nabla \cdot (\boldsymbol{k_0} \nabla \langle T \rangle - \rho_f C_{pf} \langle \tilde{T} \tilde{\boldsymbol{u}} \rangle) \tag{3}$$

The first term on the right hand side is the stagnant conduction by molecular diffusion. It depends on the fluid and solid phase thermophysical properties, the turtuosity of the structure and the porous medium geometry. The second term can be rewritten as

$$-\rho_f C_{pf} \langle \tilde{T} \tilde{\mathbf{u}} \rangle \equiv \boldsymbol{k_d} \cdot \nabla \langle T \rangle \tag{4}$$

Here, the tensor, $\boldsymbol{k_d}$, is called thermal dispersion conductivity. Correspondingly, thermal dispersion diffusivity for axial transport is defined as

$$\varepsilon_d = \frac{k_d}{\rho_f C_{pf}} \equiv -\frac{\langle \tilde{T} \tilde{u} \rangle}{\dfrac{\partial \langle T \rangle}{\partial x}} \tag{5}$$

It can be seen that the thermal dispersion diffusivity, ε_d , is determined by the spatial average of the correlation between spatial variations of temperature and velocity.

In order to obtain this correlation, one can choose a R.E.V., locate with a high spatial resolution a number of probes for temperature and velocity measurements within it, then take their readings simultaneously. Afterwards, one can calculate the spatial average quantities over the R.E.V. at any instant in time and the spatial variations at any instant in time and any particular location. The needed term $< \tilde{u}\tilde{T} >$ is computed by spatially averaging $\tilde{u}\tilde{T}$. Note that it theoretically is a function of time since no time averaging has been done. This proposed experimental method cannot be realized.

In contrast to the spatial average technique used in porous media is the evaluation of turbulence quantities taken in free and wall-bounded flows (but not porous media) in which a time-average is used to characterize the turbulence field. Any quantity can also be defined as the sum of the time-averaged value integrated over a time period sufficiently large relative to the characteristic time scale of the fluid flow situation, and a temporal fluctuation value.

$$W = \overline{W} + W' \tag{6}$$

W' is a function of time and space and $\overline{W}$ is a function of space, only.

These time-averaged quantities can be measured for an open flow by locating a probe at individual points in space and recording the readings continuously in time. This type of measurement is frequently taken. This raises the question, "Is it possible to use time-averaged values to describe the needed volumetric-averaged values?" Efforts have been taken to make a connection mathematically between volumetric-averaged quantities and time-averaged quantities.[12] Combining Eqs. (2) and (6) allows writing the volumetric average value, <*W*>, decomposed into the volumetric average of the time averages and temporal fluctuation terms as follows,

$$\langle W \rangle = \langle \overline{W} + W' \rangle = \langle \overline{W} \rangle + \langle W' \rangle \tag{7}$$

where $\langle W' \rangle$ may be a function of time but the temporal variation of $\langle W' \rangle$ would be small if time and space scales for averaging are large enough relative to turbulent eddy passing time scales and turbulence length scales, respectively. The spatial variation of any quantity W can be written as,

$$\tilde{W} = W - \langle W \rangle = \overline{W} + W' - (\langle \overline{W} \rangle + \langle W' \rangle) \approx \overline{W} - \langle \overline{W} \rangle + W' \tag{8}$$

For the spatial variations at individual spatial points, it is assumed that time and space averaging is commutative. We note that $\langle W \rangle$ is an average of W over the representative elementary volume pore space. It could change with time but since it is a space-averaged value, it is expected to be essentially time-invariant.

Applying Eq. (8) to velocity and temperature components of the fluid phase, then applying the volume-average technique to obtain the volumetric average of the product of $\tilde{u}$ and $\tilde{T}$ inside the porous medium, one can have

$$\langle \tilde{u}\tilde{T} \rangle = \langle (\overline{u} - \langle \overline{u} \rangle + u')(\overline{T} - \langle \overline{T} \rangle + T') \rangle = < \overline{u}\overline{T} > - < \overline{u} >< \overline{T} > + < \overline{u}T' > + < u'\overline{T} > + < u'T' > \tag{9}$$

The first and second terms can be calculated from single-point experimental measurements since they do not require simultaneous measurements. In most applications, instead of $< \tilde{u}\tilde{T} >$, $\overline{< \tilde{u}\tilde{T} >}$ is of interest where the overbar represents an average over a period that is sufficiently long to capture all eddy scales of importance. If one can apply the time-average to Eq. (9), the third and forth terms go to zero. Then $\overline{< \tilde{u}\tilde{T} >}$ is reduced to the sum of three terms,

$$\overline{\langle \tilde{u}\tilde{T} \rangle} = < \overline{u}\overline{T} > - < \overline{u} >< \overline{T} > + \overline{< u'T' >} \tag{10a}$$

Similarly, for the cross-transport thermal energy transport and momentum transport:

$$\overline{\langle \tilde{v}\tilde{T} \rangle} = < \overline{v}\overline{T} > - < \overline{v} >< \overline{T} > + \overline{< v'T' >} \tag{10b}$$

$$\overline{\langle \tilde{u}\tilde{v} \rangle} = < \overline{uv} > - < \overline{u} >< \overline{v} > + \overline{< u'v' >} \tag{10c}$$

Since we are interested in the eddy transport component and believe that it is the main contributor to the cross-stream dispersion, we now focus on the cross-stream transport. As the first stage of our study, we now use the momentum transport results (Eq.(10c)) to discuss thermal transport (Eq.(10b)) by imposing Reynolds analogy, which states that momentum and thermal eddy diffusivities are nearly equal.

Because the effect of eddy transport is office dominant in the cross-stream dispersion, the knowing the eddy transport term of the cross-stream dispersion is valuable. One can conclude that the first and second terms may cancel one another. The experimental support will be shown in the Appendix. The experiment is reduced to measure

$\overline{< u'v' >}$ within the porous matrix, or $\overline{\langle u'v' \rangle}$, because the spatial and temporal averages are interchangeable. Then, Eq. (10c) allows saying,

$$\overline{\langle \tilde{u}\tilde{v} \rangle} \approx \overline{< u'v' >} = \overline{\langle u'v' \rangle} \tag{11}$$

Recognizing the difficulty of measuring $\overline{< u'v' >}$ within the matrix, one might ask "Can the measurements be done within the turbulence structure of the flow just exiting the matrix instead of within the matrix?" Turbulent flows within porous media are different from free turbulent flows or turbulent flows far downstream of porous media. In the case of free turbulent flows, the eddies are formed as a break down of a shear layer. The eddies then strain one another according to the turbulence cascade theory. In porous media, the eddies are generated continuously due to separation off local solid surfaces. In some respects, this is similar to near-wall boundary layer turbulence where production of turbulence by inner-layer bursting continuously produces turbulent eddies. A probe located within the porous medium (or a boundary layer), not only sees the decaying eddies left over from upstream, but also the eddies produced locally that might have a large contribution to the eddy transport. Llittle research has been done on presenting a physical explanation of turbulent eddy transport in porous media. Masuoka and Takatsu[13] provided the most detailed description of transport through porous media in terms of vortex transport. Vortices formed within porous media were categorized into two types: void vortices and pseudo vortices. They note that the pseudo vortices are the main contributors to thermal dispersion and play the role of long-distance (large-scale) momentum transport. We expect that they have a lifetime of at least several turnovers.

Since the pseudo vortex has a large scale it might be measured immediately downstream of the porous medium instead of within the porous medium. This is similar to the assumption of advected "frozen turbulence" in which the turbulence field is unchanged as it exits the matrix and is advected downstream. One still can capture a major contribution of dispersion due to eddy transport. As the scale of the pseudo vortex might increase with the porosity, this statement becomes stronger as we approach porosity values seen in Stirling regenerators.

Experimental Measurements

Experimental Setup

The porous medium in the present test is a simulation of a Stirling engine regenerator matrix operating under representative flow conditions. It consists of two hundred round layers of 6.3 mm x 6.3 mm square mesh (4 mesh per inch), stainless steel 304, welded screens. Each layer is a disk of 190 mm diameter. The wire diameter, d_w of the screens is 0.81 mm. The screens are stacked in such a way that each layer is rotated 45° from the adjacent layer to simulate random wire arrangement of the real Stirling regenerator. The axial spacing of the screens is such that the regenerator has 90% porosity. The screen is punched out of welded screen sheets in such a way that the location of the center of the disc is random with respect to the center of the mesh in which it resides, adding to the randomness of the matrix. A more detailed description of the porous matrix is given in Ref.14. A summary of important geometric parameters is given in Table 1. Under unidirectional, steady flow operation, the flow is introduced to the regenerator matrix through a duct of 2600 mm length and a diameter that matches the disk diameter of 190 mm. The flow in this duct is mixed so that the velocity distribution of the entry flow is flat. A triple-sensor, hot-film anemometer probe (TSI 1299BM-20) is located downstream of the regenerator matrix exit plane. The experimental setup is described in Fig. 1. Three velocity components, u, v and w, are measured, for various radial positions from -38 mm to 38mm ($\pm$ 1.5 inch) about 0.0, which is the radial center of the matrix. A sampling frequency of 10kHz is used. By doing so, the turbulent shear stress, $\overline{u'v'}$, can be evaluated. To create a radial velocity gradient, $\frac{\partial \bar{u}}{\partial r}$ and a non-zero $\overline{u'v'}$, a plate with a 12.5 mm (0.5 inch) diameter orifice in the middle is inserted into the regenerator at the 20th layer of screen from the exit plane. As a result, local radial eddy diffusivity of momentum can be obtained as:

$$\varepsilon_M(r_i) = -\overline{u'v'} \Big/ \frac{\partial u}{\partial r} \tag{12}$$

where $-\overline{u'v'}$ and $\frac{\partial u}{\partial r}$ vary with position, r.

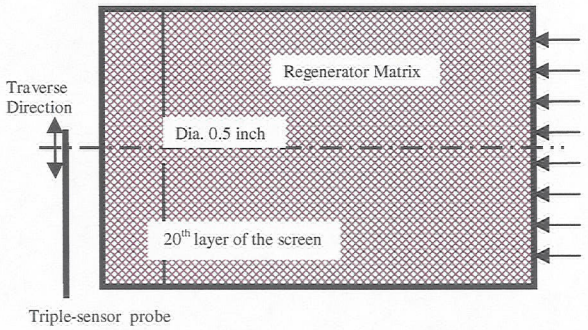

Fig. 1 Experimental Setup for turbulent transport measurements

Table 1 Geometry of the Porous Media

Parameter	Value
Wire Diameter, mm	0.8
Mesh Size, PPI	4x4
Hydraulic Diameter, mm	7.2
Permeability, m^2	$1.86X10^{-7}$
Porosity	90%

Data Processing

Figure 2 (a) shows a velocity profile at an axial location of 3.2 mm (0.125 inch) away from the exit plane of the regenerator. Due to the irregularity of the regenerator matrix, the probe might be located immediately behind a wire or immediately behind a pore. Therefore, the velocity distribution is highly variable in the radial direction, which makes it difficult to accurately evaluate the local, radial velocity gradients and the shear stress $\overline{u'v'}$. To avoid this situation attributed to the close proximity to the mesh wires, the probe is moved further away from the exit plane. The velocity profiles from 3.2 mm (0.125 inch) to 50.8 mm (2.0 inch) are shown in Fig. 2. It can be seen that the radial distribution of velocity is becoming much smoother, ensuring a more accurate evaluation of the local radial velocity gradient and shear stress, $\overline{u'v'}$.

We might expect that eddy transport in the measurement zone may differ from that immediately behind the exit plane. With all the information at the various axial locations, we are tempted to assume that the turbulent structure does not change too much within a short distance downstream of the exit plane. To check the suitability of doing this we seek a relationship between the eddy diffusivity and the axial distance from the exit plane, as $\varepsilon_M = \varepsilon_M(x)$. To eliminate the effect of randomness, only points with smooth gradients are chosen for evaluation of the averaged eddy diffusivity, $\langle \varepsilon_M \rangle$, at each axial location:

$$\langle \varepsilon_M \rangle \approx \sum_{r_i} \varepsilon_M(r_i) / N \tag{13}$$

The parameter N is the number of selected points for data processing, indicated in Fig. 2 as points with symbols in circles. As an example, the velocities at the axial location 50.8 mm (2 inches) away from the exit plane are plotted in Fig.2 i). In this case, twenty eight points are considered to be the points with smooth velocity gradients. Points with weak gradients were not processed. We find that several of the neighboring points to those eliminated (due to a weak gradient) show measured shear stress values that are of the wrong sign relative to the local mean shear, giving

a negative eddy diffusivity. We consider those points erroneous as well because, we suppose, we are not able to capture the relevant length scales of the Reynolds shear stress $\overline{u'v'}$. Points that are well inside of a continuous mean shear gradient region pass both of these tests and are processed. After these points have been eliminated, the number of selected points for evaluating the averaged values, N, is equal to 25. These are cycled points in Fig. 2 i). By similarly processing data at the other Fig. 2 planes, we can see that the number of points processed decreases significantly as the measurement plane becomes closer to the matrix exit plane.

To derive a model, we use the Prandtl mixing length hypothesis to compute the eddy diffusivity as the product of a characteristic length (taken to be the hydraulic diameter) and a characteristic velocity (taken to be the in-matrix average velocity),

$$\varepsilon_M(r_i) = \lambda d_h U \tag{14a}$$

Here, U values are the individual local velocity values at the selected points and d_h is the hydraulic diameter of the regenerator matrix. An average diffusivity coefficient is defined as,

$$\langle \lambda \rangle \approx \sum_{r_i} (\varepsilon_M(r_i) / d_h U) / N \tag{15}$$

Figures 3 a) and b) indicate the values of $< \varepsilon_M >$ and $< \lambda >$, respectively, for various axial locations.

The flow we have been measuring is that which is emerging from between the wires of the matrix. It has some characteristics of free jets. Measurements by others of eddy transport indicate that the eddy diffusivity remains constant with axial position for the near-field of axisymmetric free jets. If the present case could be modeled as an array of free jets, we may be inclined to extract from Fig. 3 a) a constant eddy diffusivity of around $1.7 \times 10^{-4} m^2/s^2$ and from Fig. 3 b) a corresponding coefficient of 0.02. We put low emphasis on the first three date points because so few of the measurements pass the two acceptance criteria described above.

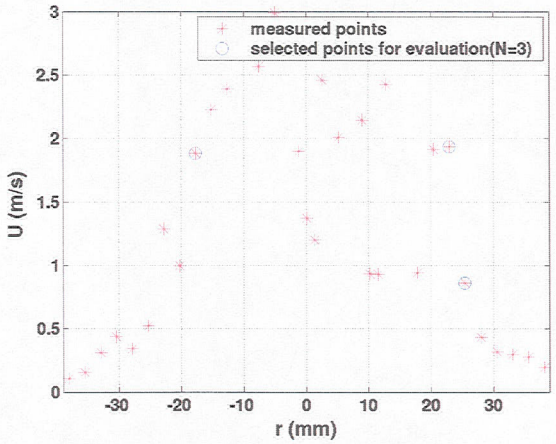

a) x= 3.2 mm (0.125 inch)

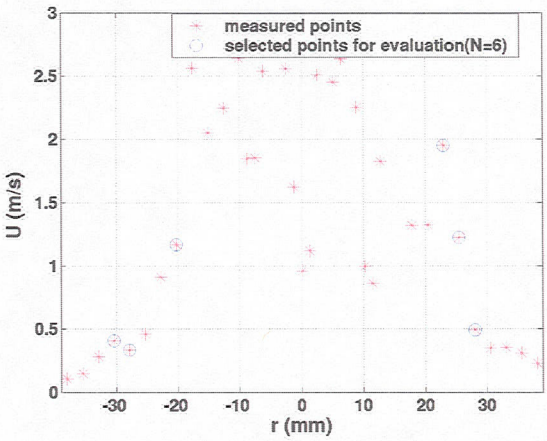

b) x= 6.4 mm (0.25 inch)

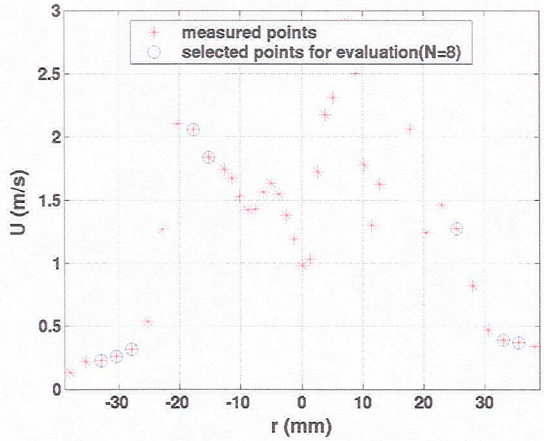

c) x= 12.7 mm (0.5 inch)

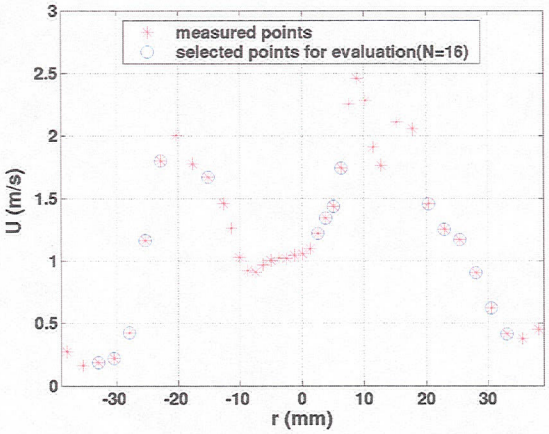

d) x= 19.1 mm (0.75 inch)

Fig. 2 Velocity Distribution at various axial locations

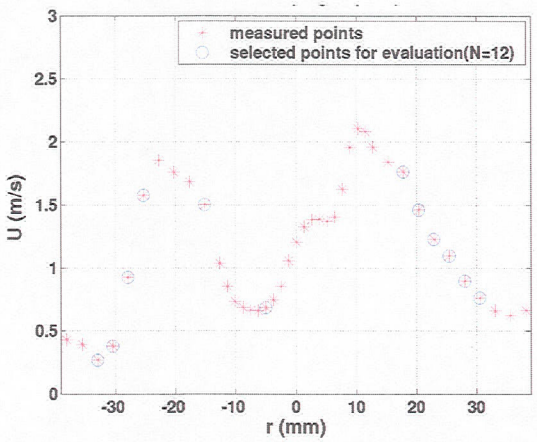

e) x= 25.4 mm (1.0 inch)

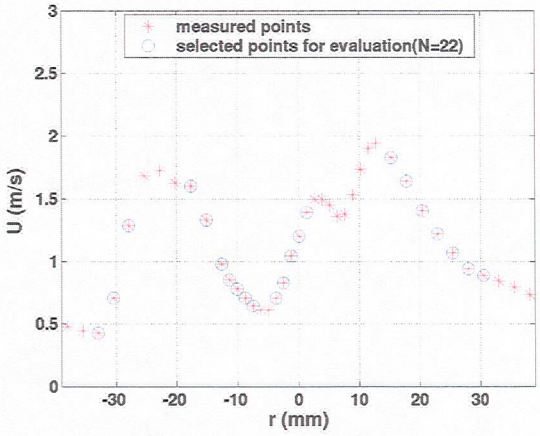

f) x= 31.8 mm (1.25 inch)

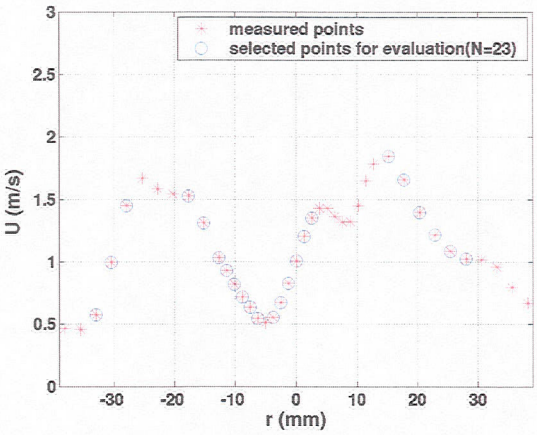

g) x= 38.1 mm (1.5 inch)

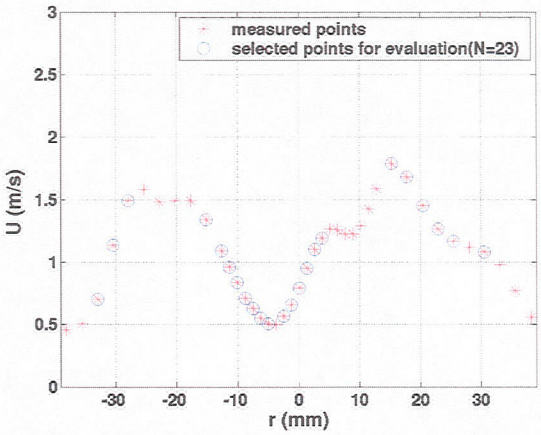

h) x= 44.5 mm (1.75 inch)

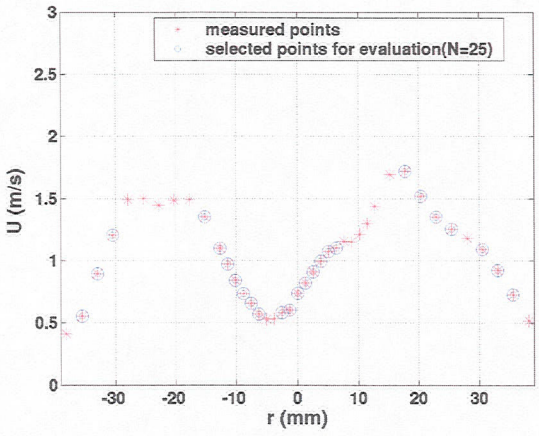

i) x= 50.8 mm (2 inch)

Fig. 2 Velocity Distribution at various axial locations

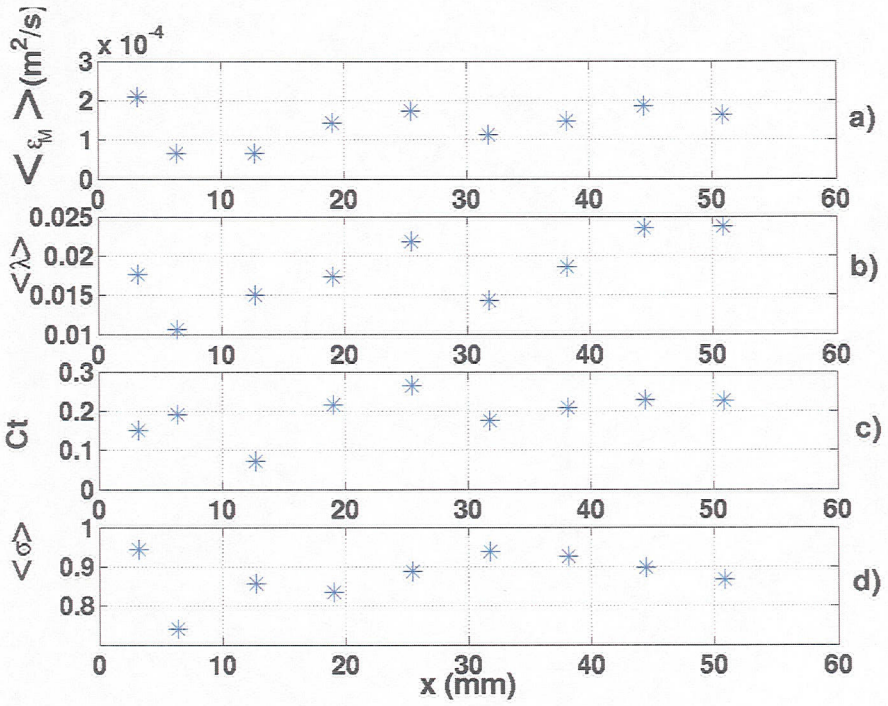

Fig. 3 Values Calculated by Eqs. (13), (15), (16) and (17)

We next test the hypothesis that, although the turbulence levels may change from within the matrix to the exit plane and beyond, the structure does not. To test this assumption with our measured data, we define a correlation coefficient and an anisotropy factor as follows

$$< \overline{u'v'} >= C_t < \sqrt{\overline{u'^2}} >< \sqrt{\overline{v'^2}} > \tag{16}$$

$$\sigma = \sqrt{\overline{v'^2}} / \sqrt{\overline{u'^2}} \tag{17}$$

If the flow structure does not change from within the matrix to the outside of the matrix, and in the immediately vicinity beyond, we might expect constant_values for these two. If so, the experiment can be reduced to measuring the correlation coefficient, C_t, and the anisotropy factor, σ, in the exit stream, and only the intensity value $\sqrt{\overline{u'^2}}$ within the matrix or at the exit plane of the matrix.

$$< \overline{u'v'} >= C_t \sigma < \overline{u'^2} > \tag{18}$$

The correlation coefficient, C_t, and σ, are computed for each x-plane. Radius-average values at each axial position using the selected points are substituted for volume averages in doing this evaluation (See Fig 3 c) and d)). This $C_t(x)$ is extrapolated to the x=0 position to give about 0.2, again with reduced emphasis on the first three data points. It is observed that a value of 0.9 for σ is maintained along the streamwise direction. This supports our previous assumption that the turbulence structure does not change in this 50 mm length (again, advected "frozen turbulence").

Discuss and Comparison

From the current experimental measurements, a model is suggested for evaluating the eddy transport component of the cross-stream dispersion in stacked wire screens or similar porous structures.

$$\varepsilon_M = 0.02 d_h U \tag{14b}$$

A comparison of the models by different researchers is given in Table 1. Since these models employ different forms and different length scales, for the purpose of comparison, all dispersion coefficients are computed based upon the hydraulic diameter of the current porous medium using the parameters listed in Table 1 for conversion and local in-pore velocity.

It can be seen that the thermal dispersion coefficients scatter widely, even for the similar porous materials. We note, however, that the modeled conditions differ from case to case, as will now be discussed.

The value from the direct measurements (Eq. (14b)), is computed from the last term of Eq. (10c) and it is assumed that the first two terms cancel. This assumption is supported by our measurements. If this assumption is not so, Eq. (14b) would be in error. Also, if the probe were too small to resolve the important scales of the turbulent flow, then $\overline{u'v'}$ and λ would be low. Studies of the scales the probe might resolve indicate that scales on the pore size should be resolved by our probe but turbulence scales on the wire size might not be resolved. These scale resolution studies were conducted in a fully-developed turbulent pipe flow in which the turbulence structure is well characterized. It appears that the larger eddies responsible for dispersion are being resolved so that filtering due to probe size is not expected to be a major problem.

Theoretical model given by Koch and Brady[6] is derived from an isotropic packed fibrous media which is the best presentation of the porous matrix in the present study. The model by Nakayam and Kumahara[7] is developed from numerical simulations using a microscopic structure of square rods. All the rods in their structure are in-line and perpendicular to the flow direction, which is similar to the aligned fibers studied by Koch and Brady[6]. Such a regular pattern might result in a reduced dispersion.

Although the model given in Sage Manual[10] for predicting dispersion in Stirling regenerator is for a similar structure of woven screens, it is derived experimentally from an overall measurement of the axial heat conduction losses[9]. It should be used for the evaluation of streamwise dispersion. The values from the study by Hunt and Tien relate to eddy dispersion near a heated wall. We know that a wall tends to suppress turbulent mixing in boundary layers so we might expect that dispersion in a near-wall region may be reduced from dispersion values which apply out in the matrix far from the wall. This may explain the smaller value than given by .

Table 2 A comparison of the thermal dispersion coefficients

Researchers	Models	Porous Media
Current researchers	$\varepsilon_M = 0.02\, d_h U$	Welded Screen
Koch and Brady[6]	$\varepsilon_M = 0.02\, d_h U$	Isotropic Fibers
Koch and Brady[6]	$\varepsilon_M = 0.0004\, d_h U$	Aligned Fibers
Nakayama and Kuwahara[7]	$\varepsilon_M = 0.0018\, d_h U$	Square Rods
Sage Manual [10]	$\varepsilon_H = 0.061\, d_h U$	Woven Screen
Hunt and Tien [8]	$\varepsilon_H = 0.0015\, d_h U$	Fibrous Media

Conclusions

An effort has been made to find a measurement technique for directly evaluating the eddy component of thermal dispersion. A relationship between thermal dispersion within a porous medium and turbulent transport in the exit flow has been discussed. The former cannot be measured with the current techniques while the latter can be measured in the laboratory. As a first step, eddy transport downstream of the regenerator matrix is measured at various axial locations. A model for the eddy component of cross-stream dispersion is derived from the experimental results. This model is compared to some other models for evaluating thermal dispersion or turbulent transport in porous structures. The comparison shows that the correlations scatter widely. However, we presented reasons why

some might not agree with others. More work is needed to directly evaluate the streamwise dispersion and eddy transport of thermal energy.

Acknowledgments

We are grateful for sponsorship of this work by the U.S. DOE Office of Energy Efficiency and Renewable Energy under the Advancement of Solar Dish/Converter Technology Initiative (DE-FC36-00G010627). Also, this work was performed for NASA Headquarters, Office of Space Science (Code S) under the Project Prometheus Program and was supported by the NASA Glenn Research Center under research grant number NNC04GA04G.

References

[1]Tew, R.C., "Overview of Heat Transfer and Fluid Flow Problem Areas Encountered in Stirling Engine Modeling," *Fluid Flow and Heat Transfer in Reciprocating Machinery*, ASME HTD-Vol. 93,Winter Annual Meeting, Boston, MA, 1987, pp. 77-88.

[2]Nield, D.A. and Bejan, A., *Convection in Porous Media*, 2nd edition, Springer-Verlag, New York, 1992.

[3]Yagi, S., Kunii, D., "Studies on Axial Effective Thermal Conductivities in Packed Beds," *A.I.Ch.E Journal*, Vol.6, 1960, pp. 543-546.

[4]Hsu, C.T. and Cheng, P., "Thermal Dispersion in a Porous Medium," *Int. J. Heat Mass Transfer*, Vol. 33, 1990, pp. 1587-1597.

[5]Metzger, T., Didierjean, S. and Maillet, D. "Optimal Experimental Estimation of Thermal Dispersion Coefficients in Porous Media," *Int. J. Heat Mass Transfer*, Vol.47, 2004, pp. 3341-3353.

[6]Koch, D. L. and Brady, J. F., "The Effective Diffusivity of Fibrous Media," *A.I.Ch.E Journal*, Vol32, No.4, 1986, pp. 575-591.

[7]Nakayama, A. and Kuwahara, "Numerical Modeling of Convective Heat Transfer in Porous Media Using Microscopic Structures," *Handbook of Porous Media*, edited by Vafai, K., Marcel Dekker Inc., New York, 2000, pp.441-488.

[8]Hunt, M. L. and Tien, C. L., "Effects of Thermal Dispersion on Forced Convection in Fibrous Media," *Int. J. Heat Mass Transfer,* Vol. 31, 1988, pp. 301-308.

[9]Gedeon, D. and Wood, J.G., "Oscillating-Flow Regenerator Test Rig: Hardware and Theory with Derived Corrections for Screens and Felts," NASA Contractor Report 198442, 1996.

[10]Gedeon, D., Sage Stirling-Cycle Model-Class Reference Guide, 3rd edition, Gedeon Associates, 1999.

[11]Kaviany, M., *Principles of Heat Transfer in Porous Media*, Springer-Verlag, New York, 1991.

[12]Lage, J. L., Delemos, M. J. S. and Nield, D. A., " Modeling Turbulence in Porous Media," Chapter 8 in *Transport Phenomena in Porous Media II*, edited by Ingham, D. B. and Pop, I., Pergamon, 2002.

[13]Masuoka, T. and Takatsu, Y., "Turbulence Model for Flow through Porous Media," *Int. J. Heat Mass Transfer*, Vol.39, No.13, 1996, pp2803-2809.

[14]Niu, Y., Simon, T. W., Ibrahim, M., Tew, R. and Gedeon, D., "Jet Penetration into a Stirling Engine Regenerator Matrix with Various Regenerator-to-Cooler Spacings," *the 1st International Energy Conversion Engineering Conference*, Paper #AIAA-2003-6014, Virginia, 2003.

Appendix

The last term of Eq. (10c) is measured directly. It is assumed that the first and second terms might cancel one another or that the sum of the two is relatively small compared to the last term in Eq. (10c). A comparison of the terms computed from the measured results at various axial locations is made in this appendix.

In order to show the relative importance between the sum of the first two terms $<\overline{uv}>-<\overline{u}><\overline{v}>$ and $<\overline{u'v'}>$, the ratio of the two is plotted in Fig. A-1. As a reminder, N data points passed the two criteria discussed above and were thus processed to evaluate the eddy diffusivity. For each of these N points, one neighbor on each side plus itself are taken as a representative pore size to compute the local spatial averaged values $<\overline{u}>,<\overline{v}>,<\overline{uv}>$ and $<\overline{u'v'}>$. It is noted that the points that are chosen as neighboring points might fall within the selected N points, or might not meet the selection criteria. In a case where all three points of the set meet the criteria, we declare it to be a good data point. As an example, for the plane x=50.8 mm, we have 15 good data points out of the 25 points. Plotted is the x-plane-averaged value of $(<\overline{uv}>-<\overline{u}><\overline{v}>)/<\overline{u'v'}>$ computed from the data and averaged over all the selected N points.

The ratio seems to be nearly zero for the x-stations where there is a sufficiently large number of good data points (further from the exit plane of the matrix). For the first three axial locations we have few good data points and the values scatter widel. For the next three, the scatter is also large and the values are much nearer zero. The last three have many more good data points than those of smaller x-value, scatter very little and are nearly zero in value. We feel that they are the most reliable data points for this evaluation. Therefore, based on these current experimental data, we can argue that the sum of the first two terms in Eq. (10c) is small relative to the term $\overline{\langle \tilde{u}\tilde{v} \rangle}$ and that the measured term $\overline{< u'v' >}$ is approximately equal to the term $\overline{\langle \tilde{u}\tilde{v} \rangle}$.

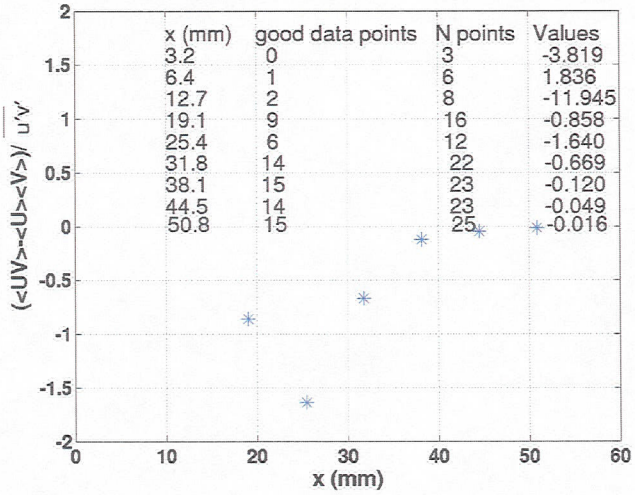

Figure A-1. $(<\overline{u}\overline{v}> - <\overline{u}><\overline{v}>) / <\overline{u'v'}>$ **at various axial locations**